INTEGRATED OPTICAL ISOLATOR

Presented by Gokhan Ozgur

Advisor: Dr. Gary Evans

July 02, 2004

Electrical Engineering - SMU

INTRODUCTION

- They are used to eliminate light that is back-reflected, from splices and connectors etc., into lasers or the EDFA's in optical telecommunication systems.

- Isolators that can be monolithically integrated with semiconductor laser waveguides were designed, and an optical isolator integratable with a semiconductor laser was fabricated and tested.

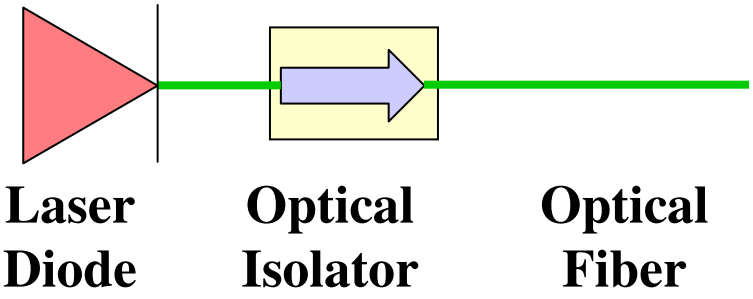

- The isolator operation is based on:
  - the nonreciprocal magnetooptic Kerr effect,
  - a novel Resonant-Layer Effect (RLE) concept [8].

MAGNETOOPTIC EFFECTS

- Gyroelectric property, the permittivity tensor of the medium:

$$\tilde{\boldsymbol{\varepsilon}} = \begin{pmatrix} \varepsilon & 0 & jQ\varepsilon \\ 0 & \varepsilon & 0 \\ -jQ\varepsilon & 0 & \varepsilon \end{pmatrix}$$

Q is the magnetooptical parameter ∝ the magnetization **M**.

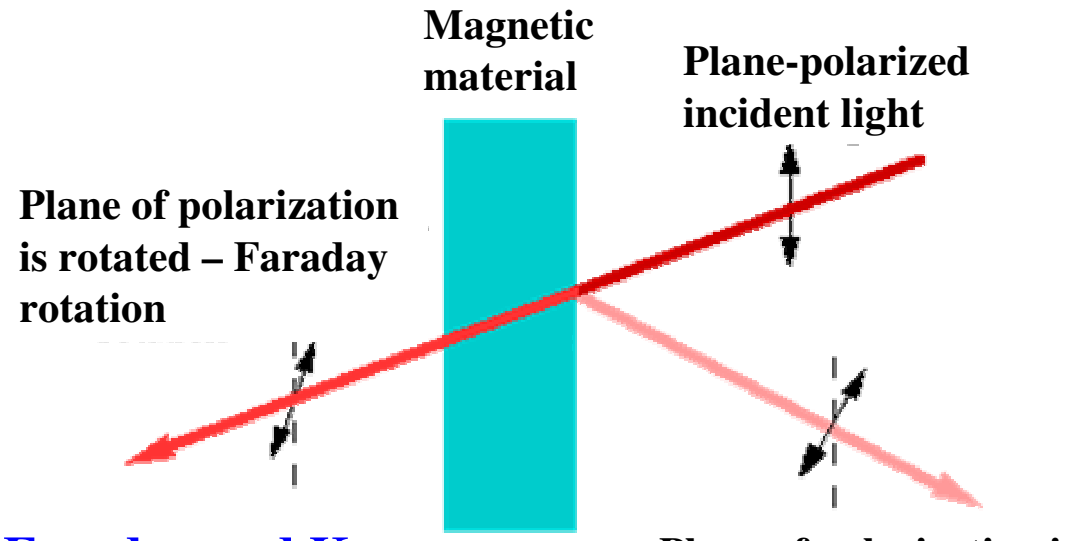

Faraday and Kerr magnetooptic effects.

- For the transverse Kerr effect case, only the power of the *p*-polarized wave (TM-mode) is affect by magnetooptical interactions at the film surface.

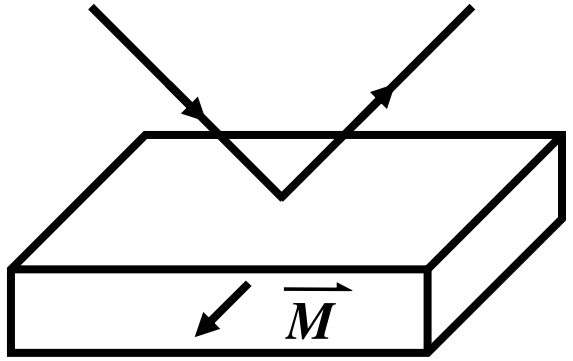

Transverse Kerr effect.

FERROMAGNETIC COMPOSITE FILMS

Evaporated or sputtered continuous ferromagnetic films have very large optical losses.

Ferromagnetic composite films are formed by introducing nanometer-size ferromagnetic particles (such as Fe, Co or Ni) in a host material (glass or semiconductor).

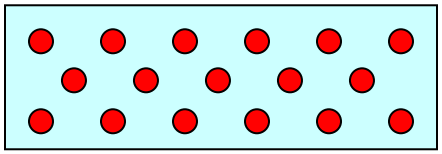

It has been experimentally demonstrated that Ferromagnetic-Plastic Composite films having Fe powder particles of about 30 nm size homogeneously dispersed in the polymer solution [1]:

- **show the magnetooptic effects as strong as the conventional films,**
- **have optical losses as low as 30 times when compared to continuous films.**

FERROMAGNETIC COMPOSITE PARAMETERS

The composite material:

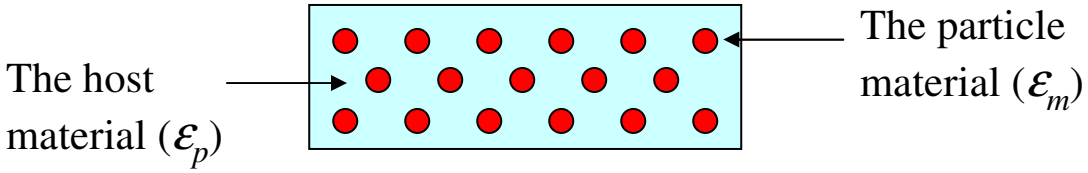

The relative effective dielectric constant of the composite:

$$\frac{\varepsilon_{eff}-\varepsilon_p}{\varepsilon_{eff}+2\varepsilon_p}=q\frac{\varepsilon_m-\varepsilon_p}{\varepsilon_m+2\varepsilon_p}$$

Maxwell-Garnet theory

The complex refractive index of the composite:

$n_c = n_{real} + i \cdot k$ will be calculated from ε_{eff}

The loss parameter and the optical modal loss for waveguide:

$$n_{loss}=\frac{2\pi \cdot k}{\lambda} \qquad \alpha=\exp\left(\frac{-4\pi \cdot WZI \cdot z}{\lambda}\right)$$

FERROMAGNETIC COMPOSITE FORMATION

- **The Ferromagnetic-Semiconductor Composite consists of nanometer-size iron particles in an InGaAsP host layer. Uniform composite profile requires multiple implantation at different energy levels.**
- **Annealing at high temperatures ~ 700 °C or more is needed to result in the formation of the clusters.**

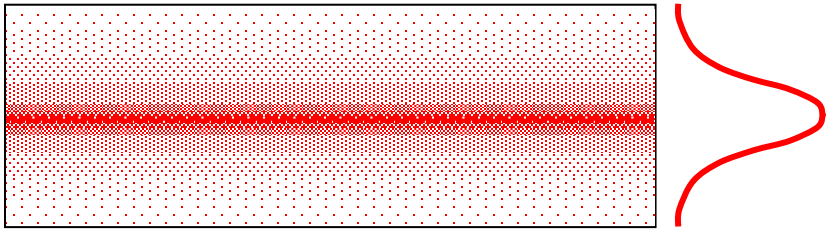

Actual implantation profile, Gaussian.

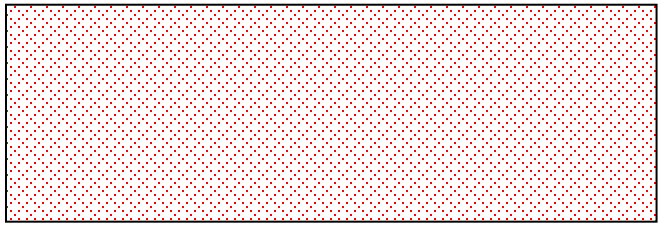

Ideal implantation profile, uniform.

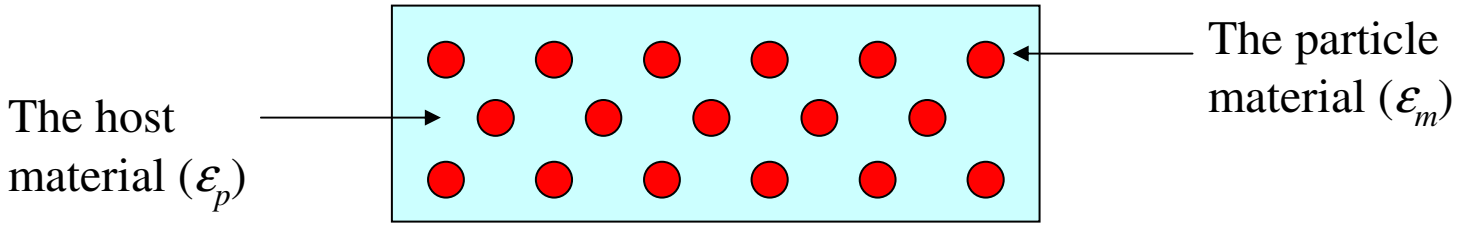

After annealing.

IMPLANT PROFILES

The implantation was performed at relatively high dose levels (~10^{16}-10^{17} /cm^2) to achieve the target Fe volume concentration of 2%. The substrate temperature was held ~20 °C during implantation. These conditions caused the InGaAsP layer to be amorphous. Some pieces have multiple implant for uniform box distribution.

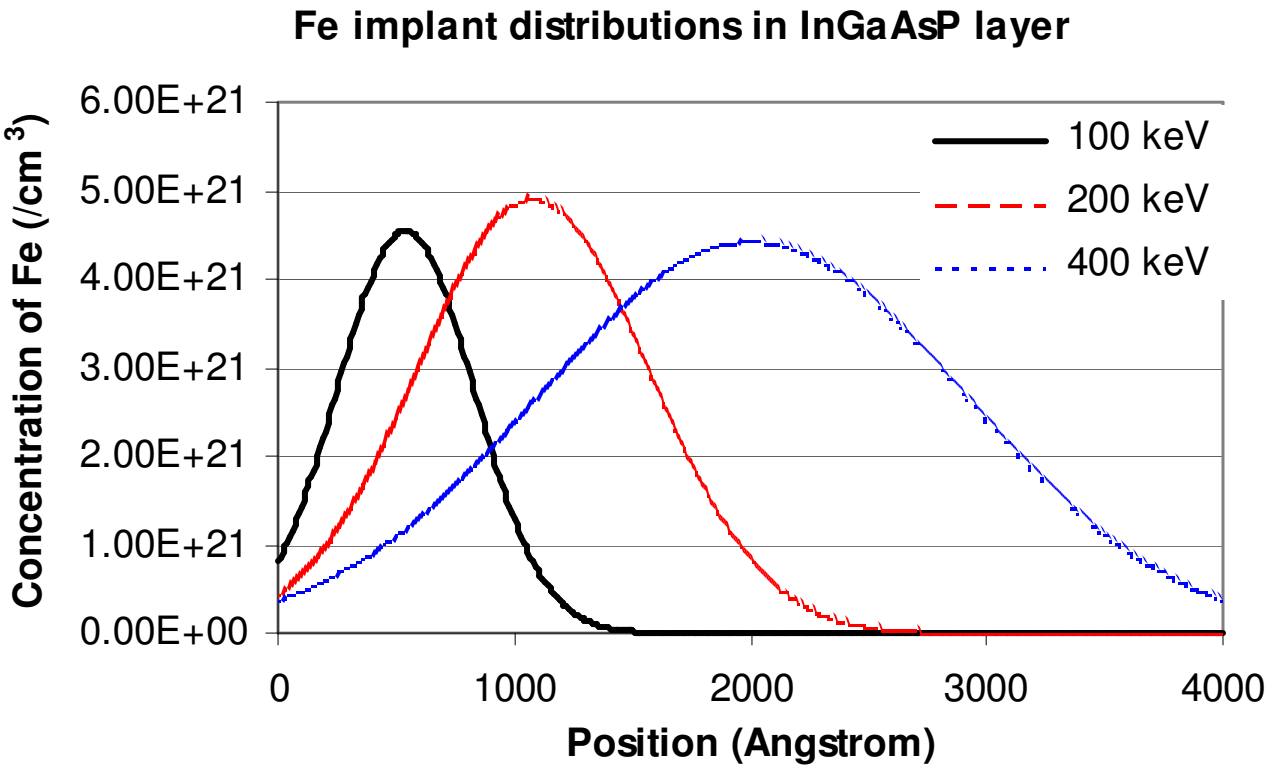

ANNEALING THE DEVICES

The solubility limit of iron in low-doped n-InP at 700 °C is about 1×10^{17} /cm^3 [7]. We assume this value for InGaAsP matrix to be somewhat similar. The Fe concentration after implantation should be enough for precipitation of Fe atoms to form nanoclusters when annealed.

The annealing will be performed:

- First, at moderate temperatures (~ 400 °C) for a long time (~ 1hr or so) to recover the crystal structure in InGaAsP. The crystal structure can be observed using x-ray diffraction.

- Next, we plan to have RTA runs at temperatures 600 – 800 °C for shorter periods to obtain the nanoparticles. The TEM images can help observe formation of nanoparticles.

RLE AND ISOLATOR SCHEMATIC

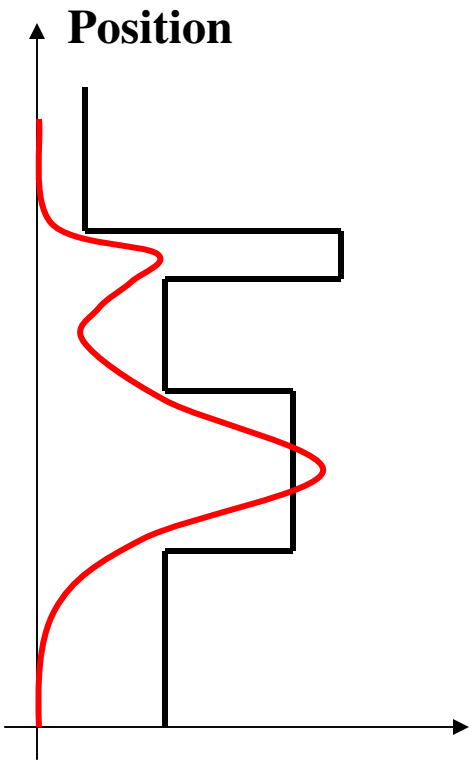

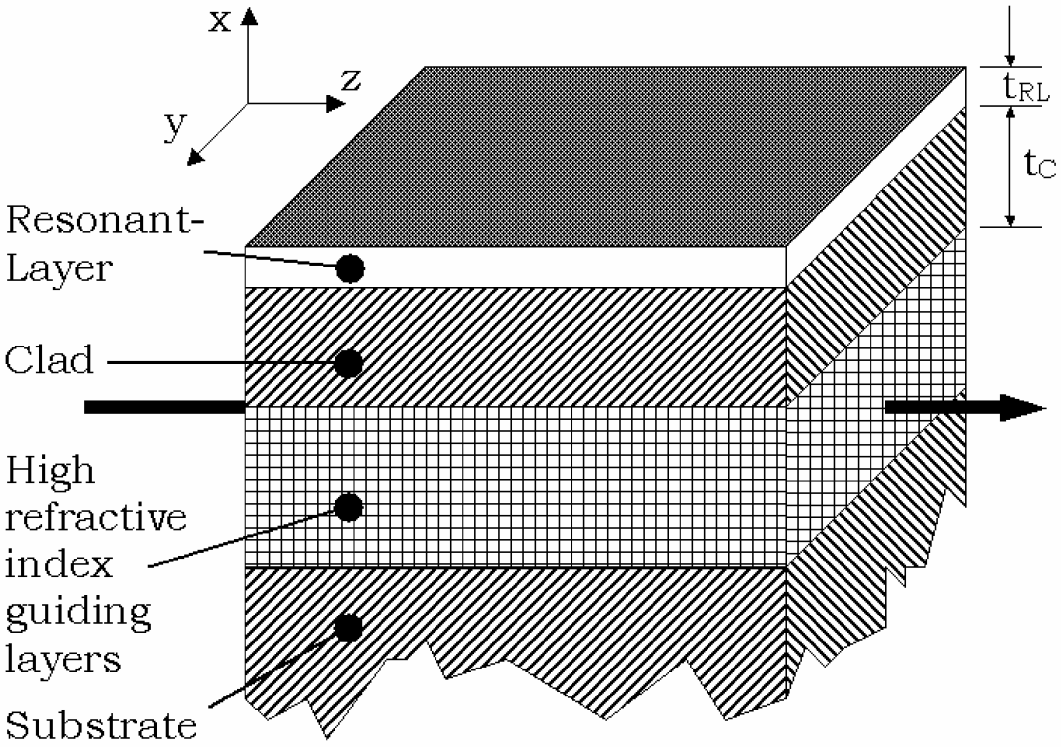

Isolator schematic.

- **A Ferromagnetic Composite layer (*Resonant-Layer*) is deposited on the clad layer of an optical waveguide (3 layer in this case),**
- **Fundamental modes' confinement in the secondary waveguide layer exhibits Resonance with proper design.**

RESONANT LAYER EFFECT

- **The secondary field amplitude is sensitive to the added layer's thickness, location, refractive index, loss, and to the wavelength of operation.**

- **A magnetic field applied in the *y* direction results large difference in loss for TM modes traveling in opposite *z* directions,**

- **This is due to a large confinement of the optical field in the RL layer in one direction, and much smaller confinement in the opposite direction.**

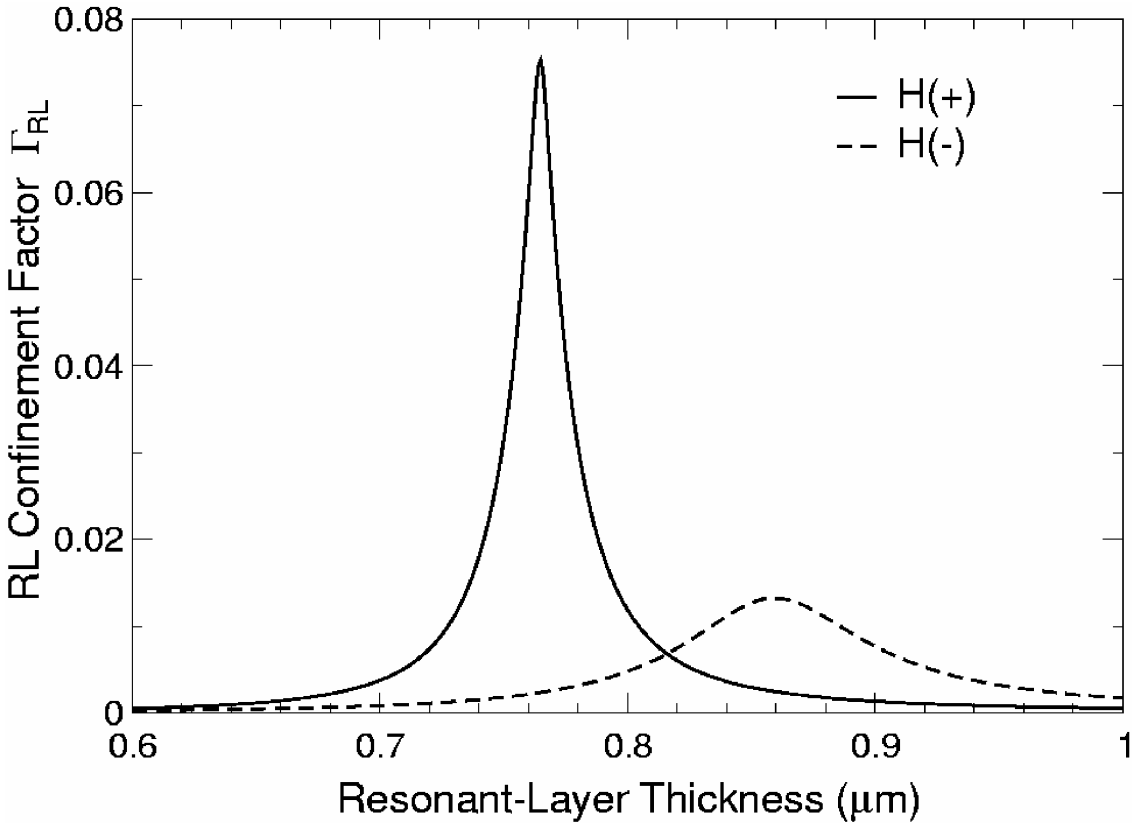

RL layer Confinement Factors.

1550-nm LASER + ISOLATOR DEVICE

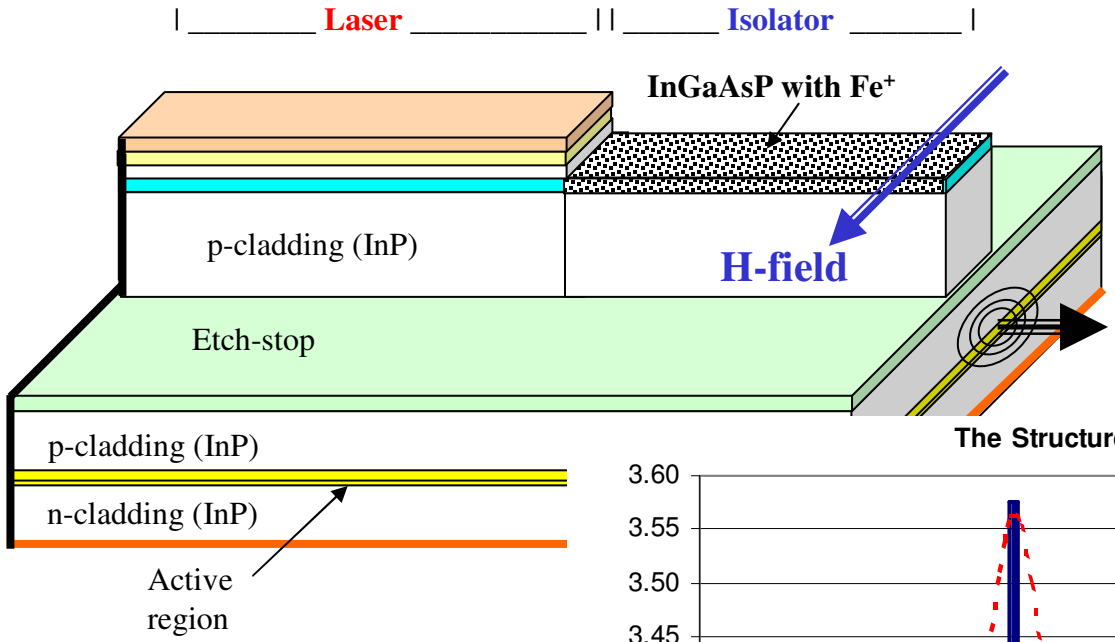

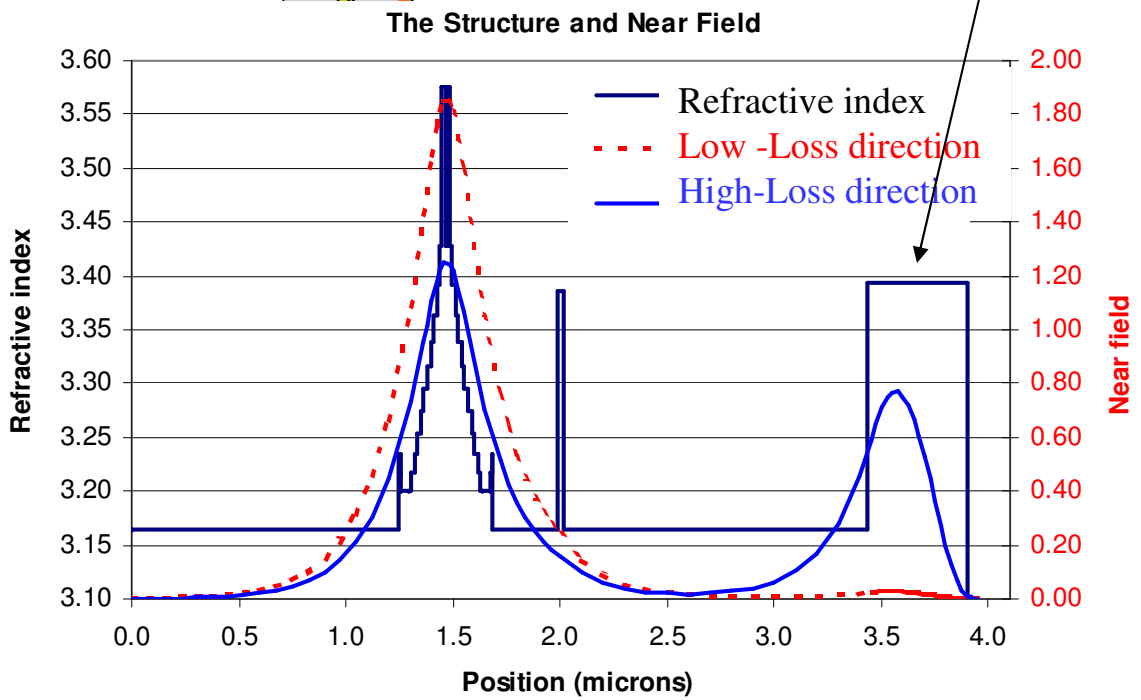

Ferromagnetic Composite Layer (InGaAsP:Fe)

- **When a static magnetic field (*H*) is applied in the *y* direction the loss and effective index for TM like waveguide modes propagating in the + *z* direction is different than for propagation in the – *z* direction.**

SMU

MAGNETIC PROPERTIES - RECALL

In the figure, magnetization (M) versus magnetic field strength (H) is shown, where M_S is the saturation magnetization (M_R) is the remanence magnetization, and H_C is the coercivity [2].

Atomic radius of Fe is 1.72 Å. Fe, Co and Ni are Group III-A elements in the periodic table.

26	27	28
Fe	Co	Ni
55.847	58.9332	58.71

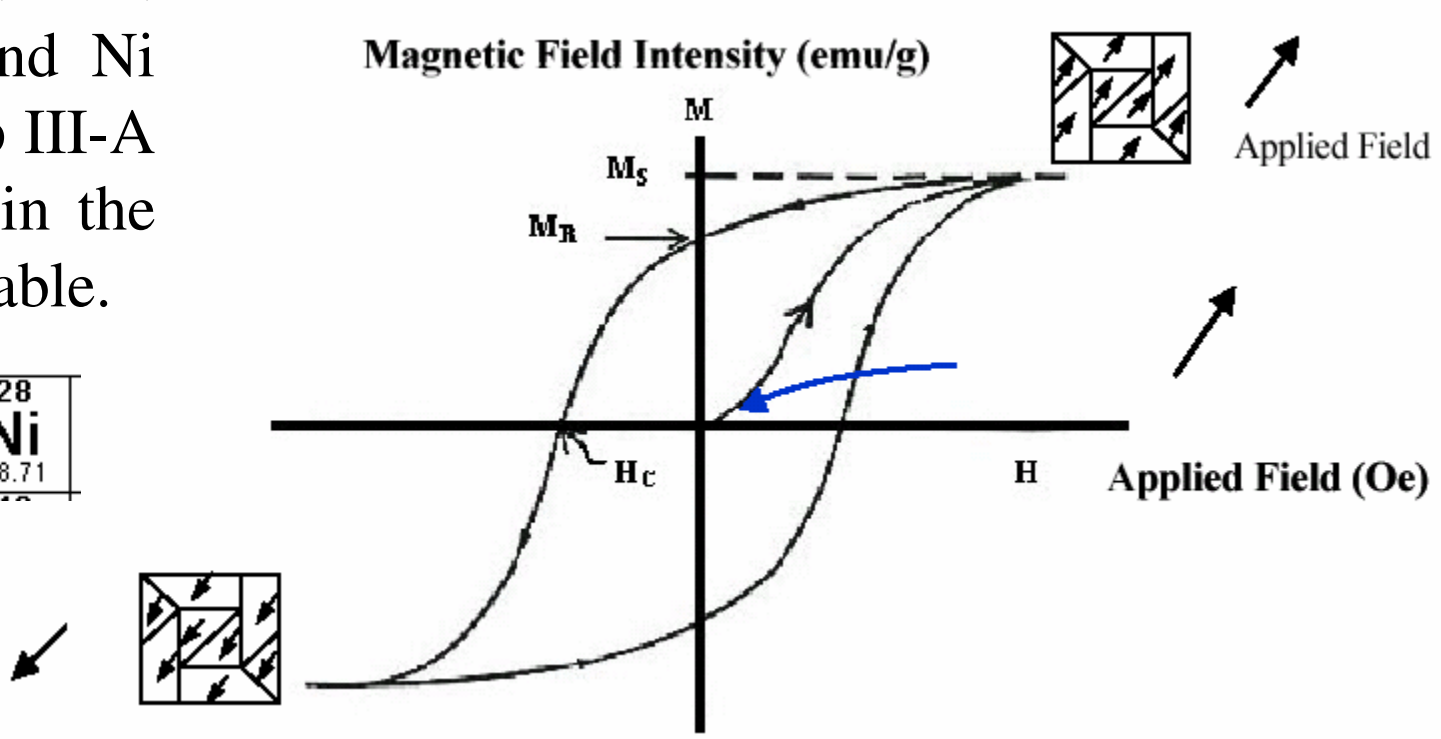

MAGNATIC DOMAINS AND DOMAIN SIZE

Ferromagnetic materials will have aligned atomic magnetic moments of equal magnitude under the applied magnetic field. They have very high permeability and high magnetization values. The estimated maximum single-domain size for spherical particles is shown in the table [2]. Also, in Ref. [3] the domain size for iron is stated about 20 nm.

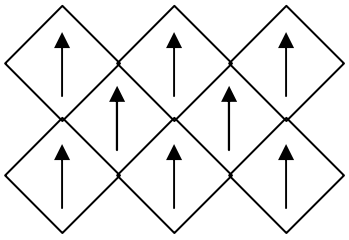

Magnetic domains

Material	D_S (nm)
Fe	14
Co	70
Ni	55
Fe_3O_4	128
γ- Fe_2O_3	166

SATURATION MAGNETIZATION

For bulk iron, the saturation magnetization is M_S=1752 gauss [4] (in cgs units 220 emu/g). The magnetization for nanoparticles increases with the particle size as shown in the table [3]. Also, we observe the drop in the coercive force H_C.

Particle size d_{core} (Å)	H_c (Oe) Experimental (T=10 K)	M_s (expt.) (emu/g)
33	2400	52.6
44	2570	37.2
84	1750	91.3
121	1425	191

PARTICLE SIZE - COERCIVE FORCE

The coercivity increases to a certain critical nanoparticle size before it drops as shown the figure [5].

A room-temperature coercivity of 1050 Oe has been observed for a 14-nm iron particles [5, ref 4], while the coercivity for bulk iron is only 10 Oe.

In [5, refs 4,6] the critical size of iron nanoparticles (where they return to superparamagnetic) is reported to be 5-6 nm at 300 °K.

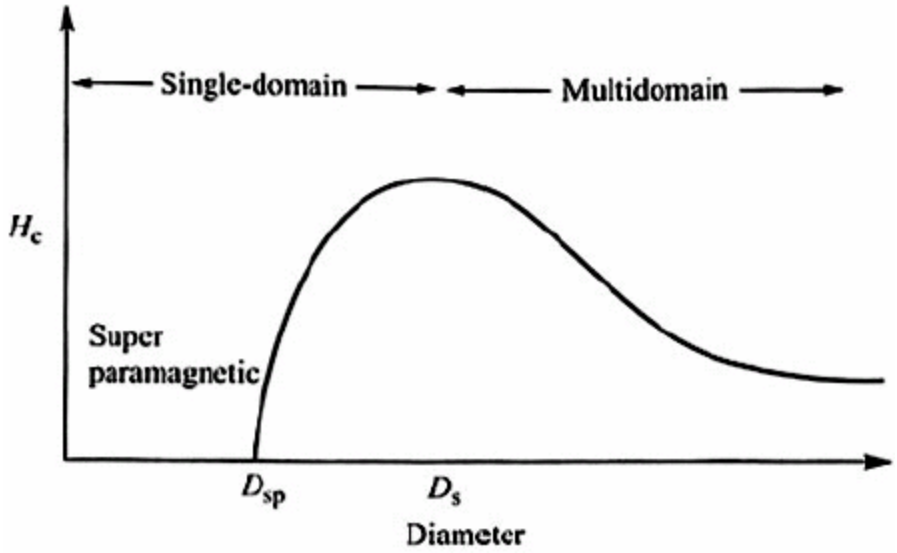

Coercivity as a function of particle size (D_{SP} is the superparamagnetic size and D_S is the single domain particle size) [2].

SMU

H-FIELD STRENGTH FOR SATURATION

The magnetic properties of ferromagnetic nanoparticles, which are in the size range of 5-10 nm, are found to be similar to those of bulk material [6].

In the table, the magnetic field to obtain saturation for iron nanoparticles in the Al_2O_3 matrix for transverse Kerr effect case is shown [6]. For the particle size of 8 nm or bigger, an external field of 5000 Gauss or less would be enough to fully saturate the material.

Nanoparticle dimensions (nm)			Fe Concentra-tion (%)	Required field strength (Gauss)	Field strength for 95% of saturation value (Gauss)	Ref. [7]
Length	Width	Height				
2.4	1.6	2.5	10	20000	~15000	Fig. 1 (d)
4	2.6	2.7	30	12000	~8000	Fig. 1 (e)
8	2	2.7	40	5000	~2000	Fig. 1 (f)

OPTICAL AND MAGNETOOPTICAL PROPERTIES

- The diagonal and nondiagonal elements of dielectric tensor were measured for particles at different sizes, and it was shown that the optical and magnetooptical properties of particles with sizes below 3-4 nm deviate from those of bulk Fe [6].

- For 30 nm size nanoparticles, Faraday rotations of Fe and Ni were measured in a field of 3.2 kOe at wavelengths 544 – 633 nm and the magnetooptic effects have found to be as strong as those of bulk material [1] .

TESTING – INITIAL RESULTS

The setup for coupling the light from an external laser source into the isolator waveguide:

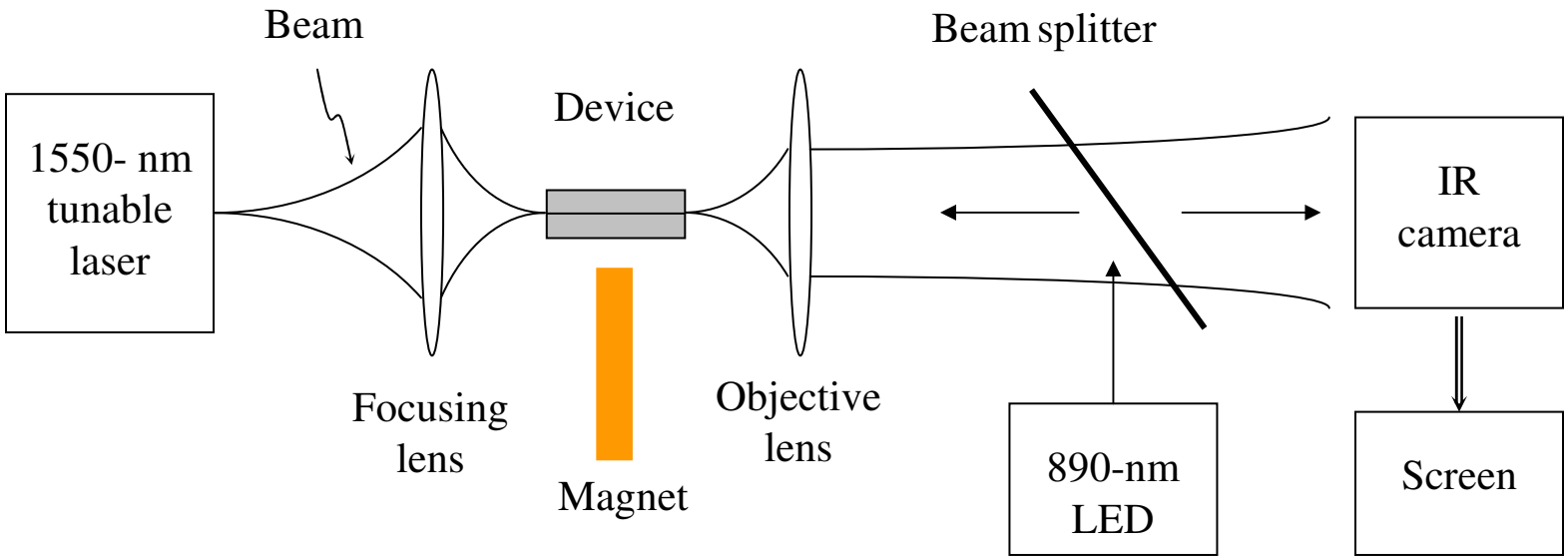

The output light from the unimplanted laser waveguide:

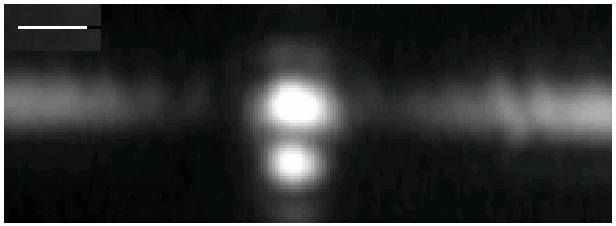

The output light from the implanted isolator waveguide:

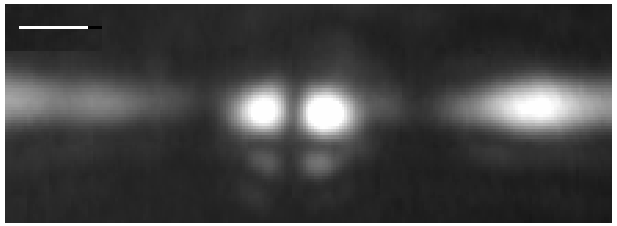

POSSIBLE REASONS

The most likely reasons that the fundamental mode was not observed in isolator waveguides were that:

- we did not anneal out the damage due to ion implantation in the Ferromagnetic Composite layer and surrounding layers,
- we did not form the magnetic nanoparticles that is necessary for the device operation,
- we did not have enough magnetic field strength to test the devices due to the high H-field requirement of nanoparticles for saturation (the old setup has a field strength of ~500 Gauss and it was not uniform either).

TESTING – COUPLING EXPERIMENT

The setup for coupling the light from an external laser source into the isolator waveguide is below. The net magnetic field strength on the device for this setup has been calculated as ~4000 Gauss.

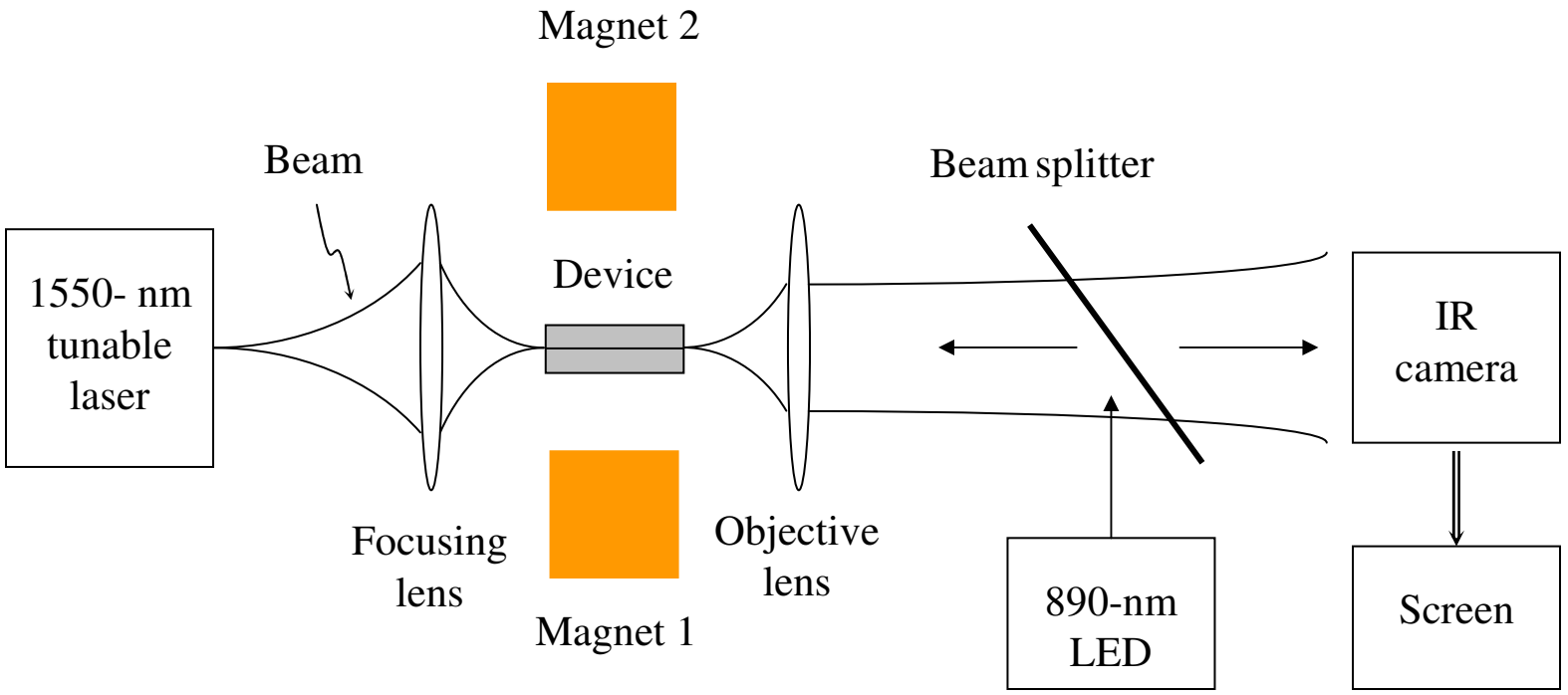

CONCLUSION – ACTION ITEMS

- The new test setup has been completed, and we are waiting for magnets and tunable laser source.
- The cleaved facets of devices (which are in bar form) have to be coated before going for annealing. PECVD SiN will be used for coating and we are considering to make a piece to hold the bars during deposition.
- The devices will be annealed at temperatures around 400 °C first and if possible x-ray diffraction will be taken.
- High temperature RTA annealing will be performed and cluster formation will be observed by TEM.
- The devices will be tested.

REFERENCES

[1] K. Baba *et al*., "Ferromagnetic particle composite polymer films for glass and semiconductor substrates", *Optics Communications*, vol. 139, pp. 35-38, 15 June 1997.

[2] Linda A. Harris, *Polymer stabilized magnetite nanoparticles and poly(propylene oxide) modified styrene-dimethacrylate networks*, PhD Dissertation, Blacksburg, Virginia, April 19, 2002.

[3] S. Gangopadhyay *et al*., "Magnetic properties of ultrafine iron particles", *Physical Review B.*, vol. 45, no. 17, pp. 9778-9787, 1 May 1992.

[4] *CRC Handbook of Chemistry and Physics*, 2002.

[5] Karine Elihn, *Synthesis of carbon-covered iron nanoparticles by photolysis of ferrocene*, PhD Dissertation, Uppsala, Sweden, 2002.

[6] J. L. Menendez *et al.*, "Optical and magneto-optical properties of Fe nanoparticles", *Physical Review B*, vol. 65, 205413, May 2002.

[7] Julian Cheng *et al*., "Semi-insulating properties of Fe-implanted InP. I. Current-limiting properties of n^+ -semi-insulating–n^+ structures", *J. Appl. Phys.*, vol. 58, no. 5, pp.1780-1786, 1 Sept. 1985.

[8] Jacob M. Hammer, Gary A. Evans, Gokhan Ozgur, and Jerome K. Butler, "Isolators, polarizers, and other optical waveguide devices using a resonant-layer effect", *Journal of Lightwave Technology*, vol. 22, no. 7, pp. 1754-1763, July 2004.